RESEARCH ARTICLE | DECEMBER 13 2018

Frequency-tunable nickel-titanium substrates for magnetoelectric sensors

Volker Röbisch; André Piorra; Rodrigo Lima de Miranda; Eckhard Quandt; Dirk Meyners

AIP Advances 8, 125320 (2018)
https://doi.org/10.1063/1.5066076

Frequency-tunable nickel-titanium substrates for magnetoelectric sensors

Volker Röbisch,[1] André Piorra,[2] Rodrigo Lima de Miranda,[3] Eckhard Quandt,[1] and Dirk Meyners[1,a]

[1]*Institute for Materials Science, Inorganic Functional Materials, Kiel University, 24143 Kiel, Germany*
[2]*Institute for Materials Science, Service Center, Kiel University, 24143 Kiel, Germany*
[3]*Acquandas GmbH, 24143 Kiel, Germany*

(Received 12 October 2018; accepted 3 December 2018; published online 13 December 2018)

We show the use of nickel-titanium (NiTi) metal thin films as functional substrates of magnetoelectric composites allowing the composites' mechanical resonance to be tuned towards the frequency range of interest by employing the gradual change of the Young's modulus during the martensite-austenite phase transformation. Such composites are successfully fabricated by layering functional piezoelectric aluminum nitride and highly magnetostrictive FeCoSiB on sputtered NiTi-films. Subsequent characterizations reveal high magnetoelectric response. Applied as magnetic field sensors a high sensitivity (with a magnetoelectric coefficient α_{ME}=290 V/cm Oe) and low limit of detection of approximately 110 pT/Hz$^{1/2}$ is observed for AC magnetic fields matching the mechanical resonance frequency. This mechanical resonance of the sensor can be altered with a Δf of 12% in the temperature interval between room temperature and 130 °C. This offers the possibility to adjust the sensor's mechanical resonance frequency featuring the highest sensitivity to the magnetic field frequency to be measured. https://doi.org/10.1063/1.5066076

INTRODUCTION

Research on magnetoelectric (ME) composites have gained in importance and their corresponding sensors have been investigated largely within the last decade.[1–3] Special attention is given to strain-mediated ME composites build as cantilevers due to their high magnetoelectric coefficient α_{ME}, which is a product property of magnetostrictive properties, the mechanical coupling and the piezoelectric properties:

$$\alpha_{ME} = \frac{\partial E}{\partial H} = \frac{1}{\varepsilon_{ii}} \times \frac{\partial P}{\partial \sigma} \times \frac{\partial \sigma}{\partial \varepsilon^m} \times \frac{\partial \varepsilon^m}{\partial H} \tag{1}$$

The magnetoelectric coefficient α_{ME} is the partial derivative of the electric field E by the magnetic field H. Here, ε_{ii} stands for the dielectric coefficient; $\partial\varepsilon^m/\partial H$ represents the magnetostrictive strain ε^m as a response to the application of a magnetic field H (piezomagnetic coefficient); $\partial\sigma/\partial\varepsilon^m$ is the mechanical coupling of the magnetostrictive strain to the stress in the piezoelectric phase and $\partial P/\partial\sigma$ describes the piezoelectric effect by the piezoelectric voltage coefficient. Due to its strain-mediated transmission the magnetoelectric effect in the magnetic field sensors leads to highest sensitivities in a narrow regime around the mechanical resonance of the sensor which for cantilever-type sensors ranges between a few hundred Hz to tens of kHz depending on their geometry.

ME composites reach outstanding record-breaking magnetoelectric coefficients, e.g. α_{ME} > 20 kV/cmOe in vacuum,[4] and explore a vast variety of applications for future technologies.[2] At the mechanical resonance of the magnetoelectric sensor the stress-mediated magnetoelectric effect increases drastically, thus the opportunity allowing to change the higher sensitivity to the actual

[a]Corresponding author: Dirk Meyners, e-mail: dm@tf.uni-kiel.de

frequency range of interest is of tremendous advantage. Due to the achieved limit of detection, which can reach values below 1 pT/Hz$^{1/2}$ in the mechanical resonance of these sensors, even applications measuring biomedical signals as in magnetoencephalography (MEG) and magnetocardiography (MCG) seem to be in reach provided that the sensor features can be transferred into the required frequency range (1 to 100 Hz) with an appropriate bandwidth. As an alternative to changing the sensor's resonance frequency, frequency conversion through AC magnetic[5,6] and electric[7] fields are introduced. This way it is possible to transfer especially low frequency signals into the sensor's working point at its resonance frequency resulting in high magnetoelectric coefficients at the low frequency of the signal. One drawback of these techniques is the application of high amplitude AC modulation fields, which lead to additional noise contributions mainly induced by the magnetostrictive component.[8,9]

Another important application is the detection of artificial weak magnetic signals at a well-defined frequency or at multiples of this signal frequency. An example of high interest is the analysis of the stimulated electric field of deep brain stimulation in case of e.g. Parkinson's disease. The electrodes for the deep brain stimulation are operated at a fixed frequency selected from a range between approximately 130 and 170 Hz.[10] Therefore, the individual tunability of the sensor's resonance is essential for a precise matching either to the stimulation frequency or their multiples resulting in a corresponding high sensitivity of the sensor.

The major aim of the presented work is to exploit shape memory alloys as a substrate for magnetoelectric composites. Using its reversible and gradual phase transformation between martensite (low Young's modulus) and austenite (high Young's modulus) the thereby altered resonance frequency is expected to allow the frequency adjustment over a wide range.

The most prominent shape memory alloys, NiTi-based alloys, are investigated as a substrate material instead of the commonly used silicon. Shape memory thick films of NiTi-based alloys (up to 80 μm) can be fabricated in a wide variety of different designs as free-standing materials,[11] i.e. for miniaturized sensor arrays. In this way freestanding NiTi cantilever beams with temperature-induced phase transformations can be combined with functional magnetoelectric layers. But also more features for NiTi are conceivable for these composites. For instance, NiTi benefits by alloying with copper for low-fatigue behavior in high numbers of cycles.[12] Additionally, by changes of the NiTi-X composition the transformation temperature hysteresis can be reduced (with X=Cu[13]). Also, the transformation temperatures can be increased by substitution of Ni with Pd or Ti with Hf to match the requirements of the application.[14,15]

The dependency of the Young's modulus on the resonance frequency for elongated cantilever beams with top coating is investigated by Negahban in Ref. 16. The center of mass y_{cm} and the inertia I_{NiTi} and I_F of the beam layers are shifted with increasing thickness of the deposited layers:

$$y_{cm} = \frac{E_{NiTi}h_{NiTi}^2 + E_F(2h_{NiTi}h_F + h_F^2)}{2E_{NiTi}h_{NiTi} + 2E_F h_F} \tag{2}$$

$$I_{NiTi} = \frac{wh_{NiTi}^3}{12} + wh_{NiTi}\left(y_{cm} - \frac{h_{NiTi}}{2}\right)^2 \tag{3}$$

$$I_F = \frac{wh_F^3}{12} + wh_F\left(\frac{h_F}{2} + h_{NiTi} - y_{cm}\right) \tag{4}$$

with E_{NiTi} and h_{NiTi} as well as E_F and h_F being the Young's modulus and the thickness of the substrate and the film, respectively. The contribution of adhesion and seed layers to the beam's stiffness is neglected. The width w is the same for all layers.

Negahban et al. derive the following formula which can be utilized to estimate the resonance frequency of the produced ME sensors with NiTi substrates and their corresponding phases:

$$f_r = \frac{1}{2\pi} \times \frac{\lambda^2}{L^2} \times \sqrt{\frac{E_{NiTi} \times I_{NiTi} + E_F \times I_F}{(\rho_{NiTi} \times A_{NiTi} + \rho_F \times A_F)}} \tag{5}$$

with $\lambda = 1.8754$ for the first bending mode.

Here, L represents the free-standing length of the cantilever, whereas ρ and A are the density and the cross section of the NiTi substrate and deposited films, respectively. For this model, the Young's

TABLE I. Parameters used for calculations of the resonance frequency model.

density NiTi ρ_{NiTi}	6450 kg/m^3
density FeCoSiB $\rho_{FeCoSiB}$	7180 kg/m^3
density AlN ρ_{AlN}	3300 kg/m^3
Young's modulus austenitic NiTi	83 GPa
Young's modulus martensitic NiTi	41 GPa
Young's modulus FeCoSiB	150 GPa
Young's modulus AlN	310 GPa

modulus and the density of the film are taken as thickness weighted averages of the two functional layers, the piezoelectric AlN and the magnetostrictive FeCoSiB. With the data given in Table I, a Young's modulus of E=83 GPa[17] for austenite (A) and E= 41 GPa[17] for martensite (M), the calculated frequency shift is in the order of 28% of the later.

MATERIALS AND METHODS

Onto a wafer with a pre-structured sacrificial material the following layer stack NiTi 50 μm/Ta 28 nm/FeCoSiB 2 μm/Ta 28 nm/Pt 150 nm/AlN 1 μm/Pt 100 nm is sputter-deposited. After structuring using photolithography and wet etching the cantilever sensors, of dimensions of 2.5 x 15 mm^2, are released from the wafer by removing the sacrificial layer. The as-sputtered amorphous NiTi has to be crystallized in a following temperature treatment step, but the non-crystallinity of FeCoSiB has to be maintained in order to preserve low magnetic anisotropy and thus a high magnetoelectric response. For this purpose, NiTi is crystallized by rapid thermal annealing (RTA) for 30 minutes at comparably low temperature[18] T=450 °C to enable phase transformation from martensite to austenite. The crystallization is done after complete stack deposition as to ensure low surface roughness during FeCoSiB growth. The amorphous structure of FeCoSiB was verified by X-ray diffraction after RTA treatment.

Subsequent magnetic field annealing at 250 °C and 0.1 T is done to set the magnetic anisotropy 90° to the long cantilever axis. During ME measurements the magnetic field is applied along the long cantilever axis and thus perpendicular to the magnetic anisotropy. The sensors are glued with a cyanoacrylate polymer to a PCB. The free-standing cantilever length is L=10 mm.

Aluminum nitride in the Ta/Pt/AlN/Pt layer sequence[19] serves as piezoelectric film in plate capacitor configuration. Its upper electrode, which is located on the freestanding part of the cantilever starting from the clamping point, has dimensions of 2 x 5 mm^2 and a capacitance of C=1.20 nF.

The magnetoelectric characterization and determination of the smallest detectable magnetic field (limit of detection, LoD) is performed in a magnetically and electrically shielded environment using a Kepco bipolar BOP 36-6ML power supply for DC magnetic biasing, a Keithley 6221 Source Meter for generation of AC magnetic field and a Stanford Research Systems SR-830 Lock-In Amplifier for ME voltage read-out. The characterization setup is explained in more detail in Ref. 6.

For the measurement of the frequency shift the capacitance and its phase angle are read out by an impedance analyzer (Agilent 4294A). Using the piezoelectric effect, the capacitance can be utilized to monitor the mechanical resonance. As the phase angle peaks the mechanical resonance is reached. In order to control the sensors temperature, the experiment is conducted in a temperature chamber. The temperature is monitored by means of a thermocouple and a PT100 thermometer, which is attached to an identically constructed reference cantilever.

Differential scanning calorimetry (DSC) measurements are performed on a PerkinElmer Pyris 7 to determine the phase transitions temperatures. DSC data are recorded between 22 °C and 102 °C at a typical rate of 10 K/min.

RESULTS AND DISCUSSION

In initial experiments the general properties of ME layers on NiTi substrates are characterized. Especially, the sensors properties at room temperature; e.g. mechanical resonance, optimal magnetic bias field, ME coefficient α_{ME} and LoD; are determined to reveal the sensor's optimal working

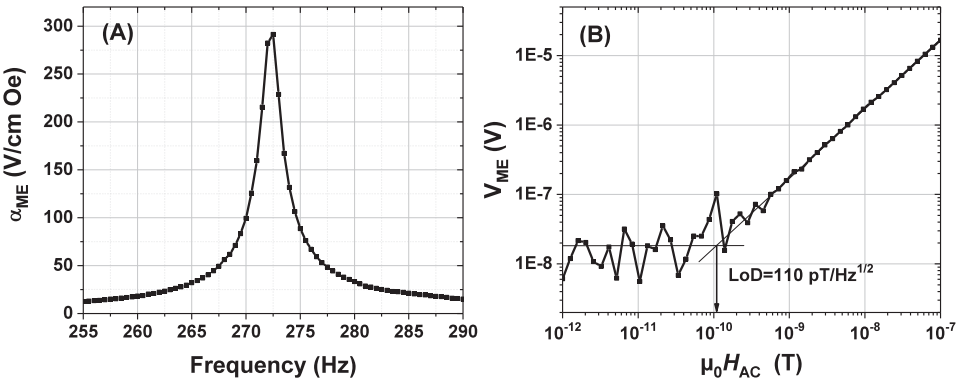

FIG. 1. AlN (1 μm)/FeCoSiB (2 μm)/NiTi (50 μm) thin film composites: (A) Magnetoelectric coefficient α_{ME} at the mechanical resonance (1st bending mode). The magnetoelectric composite reaches an α_{ME} of 290 V/cm Oe at 273 Hz. (B) Magnetoelectric voltage in dependence to the AC magnetic field. LoD of 110 pT/Hz$^{1/2}$ at the mechanical resonance.

point. Fig. 1 (A) shows the ME response as the ME coefficient α_{ME} relating to the frequency of the AC magnetic agitation signal. A DC magnetic bias B_{DC}=1.88 mT is applied along the long cantilever axis leading to a maximum ME effect. The amplitude of the AC magnetic field is chosen to B_{AC}=100 nT. The α_{ME} reveals a narrow peak with α_{ME} =290 V/cm Oe at the cantilever's mechanical resonance of f=273 Hz. In a second investigation the sensor is tested for its LoD by decreasing the AC magnetic signal B_{AC} in the range of B_{AC}= 1e-7...1e-12 T. As the B_{AC} reduces (from right in Fig. 1 (B)) there is a linear correspondence to the read-out ME voltage V_{ME} until it reaches the noise floor where the ME voltage is not related to the AC signal. The cross-over of the linear correspondence and the average noise floor determines the smallest detectable field of LoD=110 pT/Hz$^{1/2}$, demonstrating the capability of the here presented ME composite on a flexible NiTi substrate.

The shown ME characterization proves the feasibility to utilize sputter-deposited freestanding NiTi films as a substrate material for ME composite sensors. The measurements show the resonance enhancement of cantilever beams in the frequency sweep (Fig. 1(A)). The limit of detection is approximately two orders of magnitude declined compared to similar ME sensors fabricated on Si cantilevers,[19] which can be related to a lower quality factor of the substrate and to a higher roughness of the phase transforming substrate, which potentially leads to magnetic losses in the FeCoSiB. Furthermore, the α_{ME} versus magnetic field loops (not shown) indicate a broader magnetic hysteresis as expected for amorphous FeCoSiB after the RTA of the NiTi. Hence, it is assumed that temperature induced changes of the FeCoSiB material slightly deteriorates the soft magnetic properties and thus the achievable LoD. A possible alternative would be the use of a more temperature stable magnetostrictive material, e.g. FeCo/TiN multilayers.[20]

DSC investigations are performed to identify the martensite, austenite and R-phase transformations upon heating and cooling. As a measure of the ongoing phase transformation the heat flow indicates their corresponding start and finish temperatures. In Fig. 2 the data plotted is chosen to start from the end of cycle no. 10 in order to exclude formation and training effects.[21] During heating the austenite starting and finish temperature are determined as A_S=75°C and A_F=84°C, resp., while during cooling the R-Phase occurs from 60°C prior to the martensitic phase which starts to form at 53°C and finishes at 42°C.

In an insulated chamber the ME sensors' temperature is controlled and monitored during the capacitance measurements. During stepwise heating and cooling, the measurement of frequency-dependent capacitance is used to determine the corresponding mechanical resonance. In Fig. 3(A), it is plotted relative to the sensor's temperature for the 11th temperature cycle to exclude the training effect again. In the heating process the frequency follows a monotonic reduction from 332 Hz at RT (martensitic state) until about 90 °C with f_{RES}= 320 Hz and then goes up in a step-like manner to 340 Hz at T=100 °C. With even further rising temperatures the resonance goes up to 351 Hz at T=130 °C (austenitic state). While cooling the resonance frequency drops to 312 Hz during R-phase formation, before it comes back to its starting frequency of f_{RES}=332 Hz. This results in an overall resonance

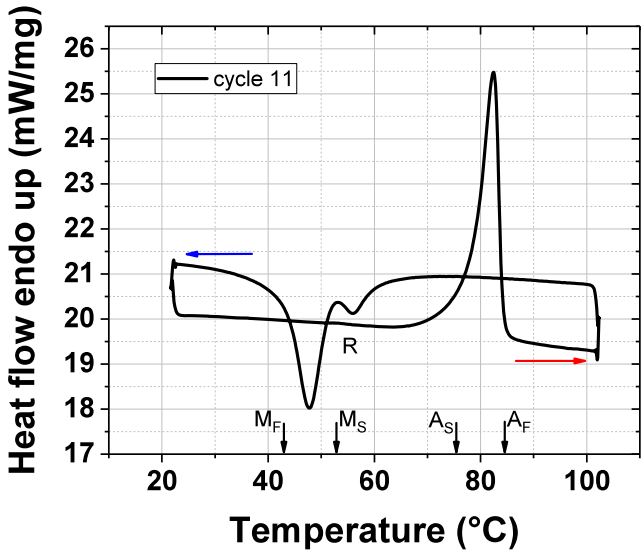

FIG. 2. Differential scanning calorimetry measurements reveal the transformation temperatures of the NiTi austenite, martensite and R-phases. The heating and cooling data is indicated with red and blue arrows, respectively. The occurrence of the R-phase as a pre-martensitic phase is noticed during cooling. The martensitic/austenitic start and finish temperatures are indicated.

frequency shift of 12% (of f_{RES} at RT) through phase transformation from martensite to austenite and back. The overshoot of the frequency drop during cooling is related to a mechanical softening of the NiTi substrate in the R-phase, as also observed for NiTi single crystals in Ref. 22. The A→R transformation hysteresis ΔT with 26 K matches perfectly in DSC and frequency investigations. However, there is a 10 K difference of the absolute phase transformation temperatures (Fig. 2 and Fig. 3(A)). This discrepancy may result from film stresses which are present in the samples and cannot fully relax by bending.

The phase transformation from martensite to austenite increases the Young's modulus and thus the mechanical resonance frequency, i.e. $E_{AUST} > E_{MART}$, with $f_{AUST} > f_{MART}$, but a linear transition is not expected. Brill et al. investigate and describe the elastic constants in NiTi single crystals and also find similar dependencies for the elasticity in between the martensite and austenite phases of NiTi.[22] Upon heating, a softening of the lattice before reaching A_F is reported, which potentially

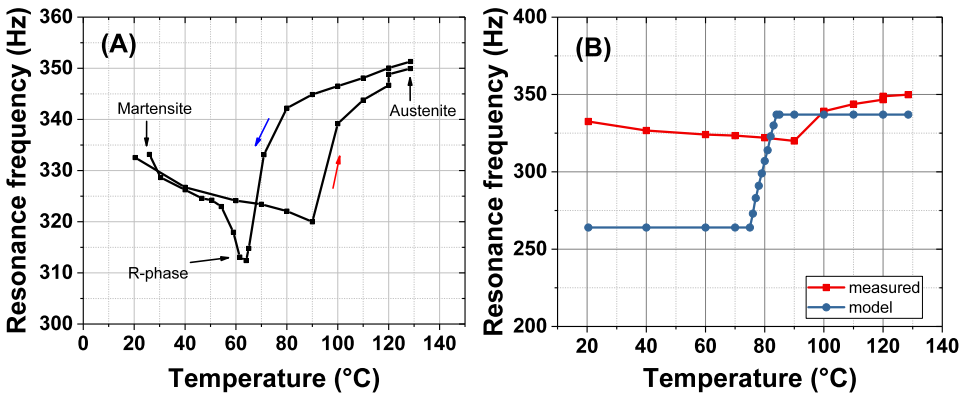

FIG. 3. From frequency-dependent capacitance measurements derived resonance frequencies plotted in dependence on the applied temperature: (A) Resonance frequency change of the ME sensor upon heating and cooling with a minimum value of 312 Hz (R-phase at 64 °C) and a maximum value of 351 Hz (austenite at 130°C). The arrows indicate the heating and subsequent cooling cycle of the shown data. (B) The right graph offers a comparison between the heating curve of the acquired data (from A) and the corresponding calculated model using equation (5) and the data summarized in Table I.

explains the decrease of f_{RES} observed here while heating in a temperature range from RT to 90°C in fig. 3a. During cooling the occurrence of pre-martensitic phases (superlattice phase and rhombohedral phase) also result in a softening of the elastic constants.

Applying equations from Eq. 2 till Eq. 5, the resonance frequency of the used sensors with martensitic NiTi (E_{MART}=41 GPa) can be calculated to f_{RES} =264 Hz, whereas with the austenitic NiTi (E_{AUST}=83 GPa) the resonance amounts to f_{RES}=337 Hz. Neglecting the aforementioned non-linearity, we now assume a simplified model (Fig. 3(B) blue dots) based on a linear change for the ratio of mixing during M→A phase transformation. It leads to a square root behavior for the frequency stroke as a function of T, resulting in a change of resonance frequency by 28% relative to the martensitic phase. The observed resonance shift (Fig. 3(B) red dots) of 12% is already sufficient to match multiples of the targeted frequency in the proposed application of deep brain stimulation, but the model promises an even higher frequency shift. At current state, the stabilization of the austenitic phase is assumed to cause a partial back transformation upon cooling due to residual austenite. Also, unrelaxed film stresses lead to a stiffening of the substrate and thus to a comparably smaller frequency shift at higher temperatures than the model predicts.

CONCLUSION

In summary, we show the applicability of freestanding NiTi metal films as possible substrates of magnetoelectric sensors allowing the sensor's mechanical resonance to be tuned towards the frequency of interest. The mechanical resonance is altered by 12% of the initial frequency at room temperature. Making use of the phase transformations from martensite to austenite and R-phase (with its Young's modulus being even 13% smaller than for martensite), the NiTi substrate varies the sensor's resonance frequency due to a change of the elastic modulus. For the sensors the limit of detection (LoD) is already as low as 110 pT/Hz$^{1/2}$. Further research, implying crystallization treatment optimizations, temperature cycling and application of temperature pulses, will boost this approach and reveal new applications fields.

ACKNOWLEDGMENTS

The authors acknowledge the financial support by the German Research Foundation DFG through the Collaborative Research Center SFB 1261. We are very thankful to our colleagues Christine Kirchhof, Erdem Yarar, Patrick Hayes, Christoph Chluba and Alexander Teplyuk for assistance during sample preparation and characterizations.

[1] J. Ma, J. Hu, Z. Li, and C.-W. Nan, "Recent progress in multiferroic magnetoelectric composites: From bulk to thin films," Adv. Mater. **23**, 1062–1087 (2011).
[2] G. Srinivasan, S. Priya, and N. Sun, *Composite magnetoelectrics: Materials, structures, and applications* (Elsevier, 2015).
[3] V. Röbisch *et al.*, "Pushing the detection limit of thin film magnetoelectric heterostructures," Journal of Materials Research **32**(6), 1009–1019.
[4] C. Kirchhof, M. Krantz, I. Teliban, R. Jahns, S. Marauska, B. Wagner, R. Knöchel, M. Gerken, D. Meyners, and E. Quandt, "Giant magnetoelectric effect in vacuum," Applied Physics Letters **102**, 232905 (2013).
[5] C.-W. Nan, M. I. Bichurin, S. Dong, D. Viehland, and G. Srinivasan, "Multiferroic magnetoelectric composites: Historical perspective, status, and future directions," Journal of Applied Physics **103**, 031101 (2008).
[6] R. Jahns, H. Greve, E. Woltermann, E. Quandt, and R. Knöchel, "Sensitivity enhancement of magnetoelectric sensors through frequency-conversion," Sensors and Actuators A: Physical **183**, 16–21 (2012).
[7] P. Hayes, S. Salzer, J. Reermann, E. Yarar, V. Röbisch, A. Piorra, D. Meyners, M. Höft, R. Knöchel, G. Schmidt, and E. Quandt, "Electrically modulated magnetoelectric sensors," Applied Physics Letters **108**, 182902 (2016).
[8] S. Salzer *et al.*, "Generalized magnetic frequency conversion for thin-film laminate magnetoelectric sensors," IEEE Sensors Journal **17**(5), 1373–1383 (2017).
[9] V. Röbisch, E. Yarar, N. O. Urs, I. Teliban, R. Knöchel, J. McCord, E. Quandt, and D. Meyners, "Exchange biased magnetoelectric composites for magnetic field sensor application by frequency conversion," Journal of Applied Physics **117**, 17B513 (2015).
[10] W. M. M. Schuepbach, J. Rau, K. Knudsen, J. Volkmann, P. Krack, L. Timmermann, T. D. Hälbig, H. Hesekamp, S. M. Navarro, N. Meier, D. Falk, M. Mehdorn, S. Paschen, M. Maarouf, M. T. Barbe, G. R. Fink, A. Kupsch, D. Gruber, G.-H. Schneider, E. Seigneuret, A. Kistner, P. Chaynes, F. Ory-Magne, C. Brefel Courbon, J. Vesper, A. Schnitzler, L. Wojtecki, J.-L. Houeto, B. Bataille, D. Maltête, P. Damier, S. Raoul, F. Sixel-Doering, D. Hellwig, A. Gharabaghi, R. Krüger, M. O. Pinsker, F. Amtage, J.-M. Régis, T. Witjas, S. Thobois, P. Mertens, M. Kloss, A. Hartmann, W. H. Oertel, B. Post, H. Speelman, Y. Agid, C. Schade-Brittinger, and G. Deuschl for the EARLYSTIM Study Group, "Neurostimulation for Parkinson's disease with early motor complications," N Engl J Med **368**, 610–622 (2013).

[11] R. Lima de Miranda, C. Zamponi, and E. Quandt, "Micropatterned freestanding superelastic TiNi films," Adv. Eng. Mater. **15**, 66–69 (2013).
[12] C. Chluba, W. Ge, R. Lima de Miranda, J. Strobel, L. Kienle, E. Quandt, and M. Wuttig, "Ultralow-fatigue shape memory alloy films," Science, American Association for the Advancement of Science **348**, 1004–1007 (2015).
[13] S. Miyazaki, T. Hashinaga, and A. Ishida, Thin Solid Films **281-282**, 364–367 (1996).
[14] R. Vitushinsky, S. Schmitz, and A. Ludwig, "Bistable thin-film shape memory actuators for applications in tactile displays," Journal of Microelectromechanical Systems **18**(1) (2009).
[15] E. Quandt, C. Halene, H. Holleck, K. Feit, M. Kohl, P. Schloßmacher, A. Skokan, and K. D. Skrobanek, "Sputter deposition of TiNi, TiNiPd and TiPd films displaying the two-way shape-memory effect," Sensors and Actuators A **53**, 434–439 (1996).
[16] W. Negahban, *Vibrations of Cantilever Beams: Deflection, Frequency, and Research Uses* (1999).
[17] Johnson Mattey medical components, Nitinol Technical Properties.
[18] J. A. Walker, K. J. Gabriel, and M. Mehregany, "Thin-film processing of TiNi shape memory alloy," Sensors and Actuators: A. Physical **21**(1-3), 243–246.
[19] E. Yarar, S. Salzer, V. Hrkac, A. Piorra, M. Höft, R. Knöchel, L. Kienle, and E. Quandt, "Inverse bilayer magnetoelectric thin film sensor," Appl. Phys. Lett. **109**, 022901 (2016).
[20] C. Klever, M. Stüber, H. Leiste, E. Nold, K. Seemann, S. Ulrich, H. Brunken, A. Ludwig, C. Thede, and E. Quandt, "Multifunctional FeCo/TiN multilayer thin films with combined magnetic and protective properties," Adv. Eng. Mater. **11**, 969–975 (2009).
[21] Z. Balak and S. M. Abbasi, "Influence of the Ti content, training cycles and pre-strain on the two-way shape memory effect in NiTi alloys," Materials & Design **32**(7) (2011).
[22] T. M. Brill *et al.*, "Elastic properties of NiTi," J. Phys.: Condens. Matter **3**, 9621 (1991).